, ,

Incorporation of uncertainty analysis in modeling of integrated reforming combined cycle

Lars O. Nord[*,a], Bo Gong[b], Olav Bolland[a], Gregory J. McRae[b]

[a]Department of Energy and Process Engineering, Norwegian University of Science and Technology, NO-7491 Trondheim, Norway
[b]Department of Chemical Engineering, Massachusetts Institute of Technology, Cambridge, MA 02139, USA

Abstract

A systematic approach to quantify uncertainties in an integrated reforming combined cycle (IRCC) process model employing CO_2 capture is presented. IRCC involves reforming of natural gas into a hydrogen-rich fuel which is then used as gas turbine fuel. Included in an IRCC plant is also a steam bottoming cycle. The analysis treats uncertain parameters as random variables whose probability distributions are estimated from limited existing information using entropy maximization. Uncertainties of model parameters were propagated through the process model using the deterministic equivalent modeling method as a computationally efficient alternative to Monte Carlo simulations. The method also quantifies the effect of each parameter on the total uncertainty of model outputs. The IRCC process model was evaluated in terms of four performance metrics: 1) net plant power output, 2) net plant efficiency, 3) CO_2 capture rate, and 4) CO_2 emitted per kWh of generated electricity. Simulation results showed that there was considerable uncertainty in the predicted net power output whereas the other three variables were less affected by input uncertainties. The IRCC plant was predicted to have a median net efficiency of 43.4% with a standard deviation of 0.5%, representing a loss of approximately 13%-points compared to a natural gas combined cycle plant without CO_2 capture. Results also indicated that the probability of meeting the requirement of at least 85% CO_2 capture rate for the plant was approximately 95%. Parameters with the largest impact on uncertainties of power output and efficiency predictions proved to be gas turbine inlet temperature, and compressor and turbine efficiencies. For the CO_2 emissions, the equipment pressure drop and the steam-to-carbon ratio proved important. Therefore, the focus of future work should be to reduce uncertainties in these parameters in order to improve the confidence of the IRCC model.

Key words: uncertainty analysis, carbon capture and storage (CCS), process modeling, pre-combustion capture, deterministic equivalent modeling method (DEMM), integrated reforming combined cycle (IRCC)

---

*Corresponding author
Email address: lars.nord@ntnu.no (Lars O. Nord)

1. Introduction

Capturing the greenhouse gas CO_2 from fossil fueled power plants can be part of a mitigation strategy to attenuate climate change. There are several approaches for capturing CO_2 from power generation. Pre-combustion capture, where the fossil fuel is decarbonized to produce a syngas, is one option. The carbon, as CO_2, is separated out before the combustion takes place. For coal, pre-combustion capture could be implemented in an integrated gasification combined cycle (IGCC). IGCC plants exist, but none of them employs CO_2 capture. For natural gas pre-combustion capture, the integrated reforming combined cycle (IRCC) which reforms natural gas into a hydrogen-rich fuel, is one alternative. This technology has yet to be implemented in practice. Research and development of new energy and environmental control technologies like the IRCC, without exception, face significant challenges due to lack of experience in commercial application of such technologies. Uncertainty is likely to exist in a wide range of parameters that characterize process models, including material properties, operating conditions, and design factors. The uncertain nature of model parameters, coupled with uncertainty associated with process configuration, renders predictions of the commercial-scale performance and cost of a new technology inherently uncertain. This suggests uncertainty need to be systematically and explicitly analyzed in modeling advanced technologies in order to examine the impact on model outputs and establish confidence limits of the predictability of models. Failure to account for uncertainty often results in point estimates of performance and cost that are based on poorly calibrated data or assumed values of parameters. Such estimates are unable to capture the full spectrum of possible outputs and can sometimes have misleading implications regarding comparative analysis of alternative technologies [1].

A systematic approach is needed to explicitly characterize uncertainties in IRCC systems. Uncertainty analysis provides the means to carry out this investigation and aims to address three major issues: (1) uncertainty quantification; (2) uncertainty propagation; (3) sensitivity analysis. The primary aim of uncertainty quantification is to select a set of parameters that are subject to significant uncertainties and develop quantitative representation of their uncertainties. Uncertainty propagation implements process models with probabilistic inputs and determine uncertainties in the model predictions. Sensitivity analysis, defined in a slightly different way from convention, examines the dependence of model predictions to uncertainties in the input parameters and identifies those which contribute the most to overall uncertainties. By excluding insignificant parameters from future analysis, computational requirement can be lowered and research efforts be directed to those where reduction in uncertainty would best improve the predictive capability of the models. Uncertainty propagation is by far, among the three tasks, the most demanding one.

Conventional approach to propagation of parametric uncertainty is via Monte Carlo simulation with either simple or stratified sampling methods. In Monte Carlo simulations, each uncertain parameter is treated as a random variable and assigned an appropriate probability distribution. Samples of model parameters are drawn from their respective probability distributions and the process model is solved repeatedly to yield a set of predicted values from which the probability distribution and other statistics of model response can be inferred. Monte Carlo simulation has by far been predominantly employed in study of uncertainties associated with advanced energy and environmental control technologies [1, 2, 3, 4]. Monte Carlo simulation, however, suffers from two major drawbacks. First, computational requirement heavily depends on the number of uncertain parameters and the complexity of process models. It easily becomes intractable as hundreds of thousands of samples may be needed for models with large number of parameters. Variance reduction techniques like stratified sampling can alleviate computational burden but only to modest extent. Second, this approach does not provide direct information about the sensitivity of model outputs to specific parametric uncertainties.

To address the aforementioned problems associated with conventional methods, a comprehensive uncertainty analysis framework has been developed. It possesses the following key features: (1) quantification of parametric uncertainties by means of entropy maximization; (2) propagation of uncertainties using a computationally efficient method; and (3) determination of sensitivities of uncertain parameters. The main objectives of this paper are to demonstrate the effectiveness of the uncertainty analysis framework in process modeling and to assess the effect of parametric uncertainties on the predictions of an IRCC model. Similar process configurations have previously been studied [5, 6, 7, 8, 9, 10, 11]. Results from these studies show lower heating value (LHV) net plant efficiencies ranging from 42% to 51% and CO_2 capture rates between 80% and 95%.

The remainder of the article is divided into the following sections: Section 2 describes the details of the methodologies used in the article including a description of the process, model assumptions, and the uncertainty methodology. The results are shown and analyzed in Section 3, and concluding remarks are given in Section 4.

2. Methodology

The IRCC was modeled in GT PRO and Aspen Plus. GT PRO was used for the power plant model including the gas turbine (GT), steam turbine (ST), and heat recovery steam generator (HRSG). The Aspen Plus simulations consisted of two separate models. One included the reforming process and the water-gas shift reactors. In this model, numerous heat exchangers were included, among those the whole process pre-heating section. Air and CO_2 compression was also incorporated into the model. The other Aspen Plus model was a chemical absorption CO_2 capture process model as part of the pre-combustion setup. This sub-system was modeled as a hot potassium carbonate process. The models were linked by Microsoft Excel utilizing Aspen Simulation Workbook and the Thermoflow E-LINK. For the CO_2 capture sub-system, the model was not directly linked to Excel, instead a simple separator model, with inputs from the full capture model, was included in the reforming flow sheet. The uncertainty analysis was done in Matlab and Excel. Matlab was, not the least, used because of its strong random number generator.

The process model and its assumptions are described in Sections 2.1 and 2.2. The uncertainty method is described in Section 2.3.

2.1. Process description

The process reforms natural gas to a syngas as shown in Fig. (1). Reforming of natural gas is modeled as a two-step process. In the pre-reformer higher hydrocarbons are converted to protect against coking in the auto-thermal reformer (ATR) according to endothermic reaction (1) and exothermic reactions (2) and (3).

$$C_xH_y + xH_2O_{(g)} \rightarrow xCO + (x + \frac{y}{2})H_2 \qquad -\Delta H^0_{298} < 0\,\mathrm{kJ/mol} \tag{1}$$

$$CO + 3H_2 \rightleftharpoons CH_4 + H_2O_{(g)} \qquad -\Delta H^0_{298} = 206\,\mathrm{kJ/mol} \tag{2}$$

$$CO + H_2O_{(g)} \rightleftharpoons CO_2 + H_2 \qquad -\Delta H^0_{298} = 41\,\mathrm{kJ/mol} \tag{3}$$

The air-blown ATR is divided into a combustion zone, a thermal zone, and a catalytic zone. The heat generated in the combustion zone provides heat for the reforming in the thermal and catalytic zones. Substoichiometric methane combustion in the ATR can be represented as

$$CH_4 + \frac{3}{2}O_2 \rightarrow CO + 2H_2O_{(g)} \qquad -\Delta H^0_{298} = 519\,\mathrm{kJ/mol} \tag{4}$$

In the thermal and catalytic zones, below the combustion zone, the main reactions are the water-gas shift reaction (3) and methane-steam reforming

$$CH_4 + H_2O_{(g)} \rightleftharpoons CO + 3H_2 \qquad -\Delta H^0_{298} = -206\,\mathrm{kJ/mol} \tag{5}$$

In the high-temperature and low-temperature water-gas shift reactors (HTS and LTS) most of the the remaining CO is converted to CO_2 according to reaction (3). Due to the temperature driving force in the HTS, the shift reactor equipment size can be kept smaller. However, the conversion would be too low if only using an HTS. Therefore, an LTS with a lower temperature and a more active catalyst is needed. Downstream of the shift reactors consisting of about 90% CO_2 is separated in the CO_2 capture sub-system which is intended to removed 85% of the CO_2. The hydrogen-rich fuel vented from the absorber is used for the gas turbine. As the ATR is air-blown there will be a significant portion of nitrogen in the gas. This nitrogen is used as fuel diluent for NO_x abatement in the GT combustor. The air needed for the ATR is bled from the GT compressor discharge plenum and boosted up to system pressure with an air compressor. There are a number of heat exchangers in the system. The pre-heating of the reforming streams is handled in various zones in the HRSG. The syngas cooler, located after the ATR, acts as an evaporator for the high-pressure (HP) steam cycle. The other heat exchangers for the process streams either generate low-pressure

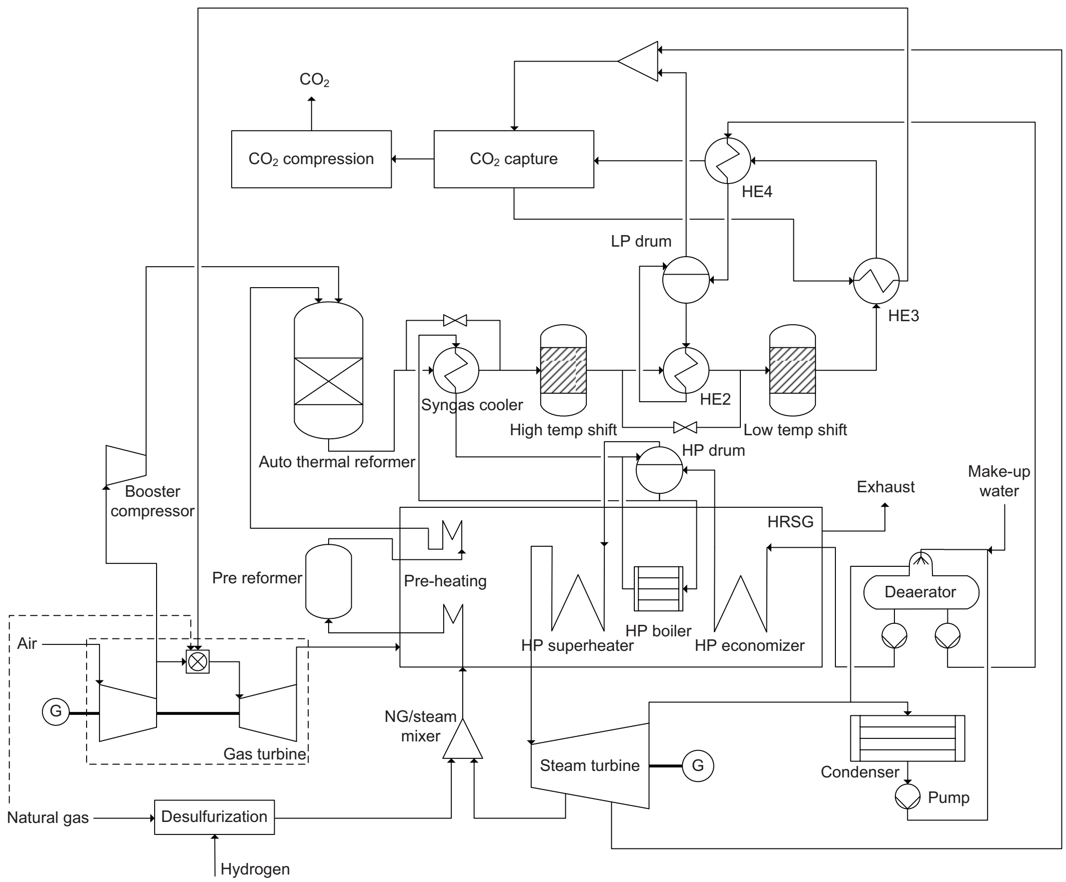

Figure 1: IRCC process flow sheet.

(LP) steam for the reboiler in the capture sub-system or pre-heat fuel for the GT. The selected gas turbine is a GE 9FB. The bottoming steam cycle, including the HRSG and a ST, is a single-pressure system at approximately 85 bar. The CO_2 capture sub-system consists of a hot potassium carbonate process. After the capture sub-system, the CO_2 is compressed to 150 bar in the CO_2 compression (4 stages) and pump train.

2.2. Process model assumptions

The process was designed with a requirement of at least 85% CO_2 capture rate. To achieve an overall capture rate of about 85% the chemical absorption sub-system was modeled for a 90% capture rate. During the simulation work it was noted that the low-pressure and intermediate-pressure sections in the HRSG became quite small because of the significant pre-heating requirements. Because of this and to simplify the process it was decided to have a single-pressure level in the HRSG. Other assumptions include ISO ambient conditions and a direct seawater cooled condenser with a condensating pressure of 0.04 bar. The natural gas composition used in the model is displayed in Table 1.

Table 1: Natural gas composition

Component name	Chemical formula	Unit	Value
Methane	CH_4	vol%	79.84
Ethane	C_2H_6	vol%	9.69
Propane	C_3H_8	vol%	4.45
i-Butane	C_4H_{10}	vol%	0.73
n-Butane	C_4H_{10}	vol%	1.23
i-Pentane	C_5H_{12}	vol%	0.21
n-Pentane	C_5H_{12}	vol%	0.20
Hexane	C_6H_{14}	vol%	0.21
Carbon dioxide	CO_2	vol%	2.92
Nitrogen	N_2	vol%	0.51
Hydrogen sulfide	H_2S	ppmvd	5

The pre-reformer and ATR are modeled as Gibbs reactors. The HTS and LTS are modeled as equilibrium reactors with restricted equilibrium based on temperature approach. The capture sub-system absorber and desorber are modeled with Aspen Plus RadFrac columns. However, in the reforming flow sheet the capture sub-system was modeled as a simple separator model with inputs such as split ratios, temperatures, and pressures from the absorption model. Outputs from the absorption model also included pump work and reboiler duty. For the simplified absorption model within the reforming flow sheet, the reboiler duty was an input rather than an output.

2.3. Uncertainty analysis

Parametric uncertainties are typically represented by probability distributions. It is therefore a major objective of the proposed uncertainty analysis framework to encode currently available information about model parameters and estimate the probability distributions of model predictions based on input uncertainties. Characterization of parametric uncertainties can be carried out using various techniques depending on the nature of uncertain variables and level of information available. Uncertainties in input parameters can be simultaneously propagated through the process models to yield estimates of uncertainties in output values. An equally important outcome is sensitivities of output uncertainties to input parameters through which controlling sources of uncertainties can be identified. A schematic diagram of the framework is shown in Fig. 2.

Uncertainty quantification

Uncertainty exists in several aspects of a new process regarding its technical performance and costs. This work focused solely on the technical performance of an IRCC process. There are several types of uncertain parameters, including material properties, equipment design factors, operating condition parameters, and performance variables. By nature, these uncertain variables fall into three categories: (1) stochasticity, variables whose values vary in an unpredictable manner. Examples include conversion rate over an reactor and isentropic efficiency of a compressor; (2) systematic and statistical error, variables with fixed values which, however, cannot be measured with perfect accuracy. Thermal chemical and kinetic parameters are

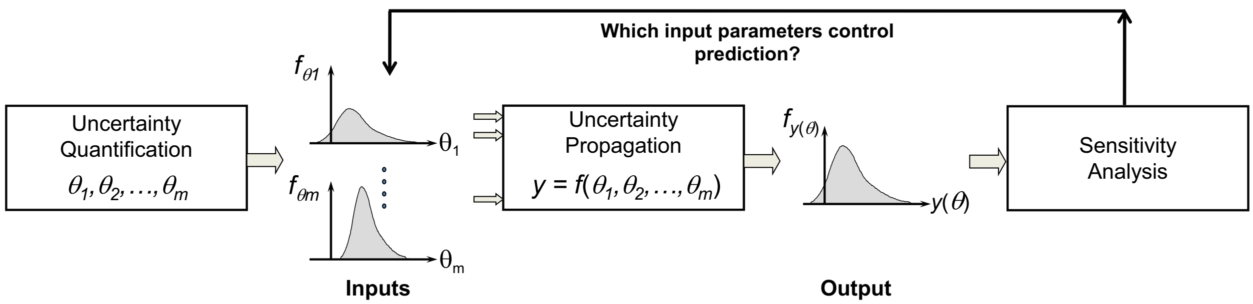

Figure 2: Diagram of the uncertainty analysis framework.

typically of this type; (3) empirical parameters lacking experimental justification. This type of variables are normally contingent on the choice of model and its assumptions. For instance, temperature approach is used to account for non-ideality in equilibrium-based reactor models. The GT turbine inlet temperature also falls within this category.

Uncertainties of different types can be quantified using different approaches. When experimental measurements are available, types 1 and 2 variables can be estimated by means of statistical inference techniques. Unfortunately there is often insufficient data for some variables, particularly for new technologies. When data are lacking, estimation of uncertainty has to rely on informed judgments of technical experts. This is specially necessary for type 3 variables whose values are difficult, if not impossible, to validate by experimentation. In this work, an information theoretic method, namely entropy maximization, was employed to encode experts' judgments regarding parametric uncertainties as probability distributions.

The information prescribed by technical experts generally pertains to descriptive characteristics of the uncertain variables, such as range, average value, most likely value, measurement error, etc. This information is typically insufficient to define a unique probability distribution. There usually exists more than one probability distribution satisfying a single set of conditions. Solution to this problem relies on the maximum entropy principle. In the theory of information, entropy S of a probability distribution $f(x)$ is a measure of uncertainty associated with $f(x)$

$$S = -\int_X f(\zeta) ln f(\zeta) d\zeta \tag{6}$$

The maximum entropy principle suggests the probability distribution that has the maximum entropy (uncertainty) permitted by the available information be used to make inference based on incomplete information. This implies any other probability distribution with less uncertainty will invoke unwarranted additional information and thus could be biased. Based on this principle, the appropriate probability distribution can be selected by maximizing the entropy in Eq. (6) subject to constraints posed by the available information. Almost all commonly used probability distributions, discrete or continuous, can be derived in this way. For example, uniform distribution has the largest entropy when only the range is known. Gaussian distribution has the largest entropy provided the mean and standard deviation are known for variables who have support on (-∞, ∞). We shall not elaborate on the derivation. More details can be found in information theory related texts [e.g., 12].

Uncertainty propagation

Uncertainties were simultaneously propagated through the IRCC process model using the deterministic equivalent modeling method (DEMM), a computationally efficient method developed by Tatang [13] as an attractive alternative approach to Monte Carlo simulation for complex models. In DEMM, parametric uncertainties are directly represented by polynomial chaos expansion of uncertain basis. For instance, a Gaussian uncertain parameter x with mean μ and standard deviation σ can be expressed by

$$x = \mu + \sigma\zeta \tag{7}$$

where ζ, a standard Gaussian random variable, represents the uncertain basis. DEMM approximates the output uncertainties as probabilistically weighted polynomials of uncertain model parameters.

$$y = \sum_{k=0}^{\infty} a_k H_k(\zeta_1, ..., \zeta_M) \tag{8}$$

where H_k are orthogonal polynomial functions of ζ_1, ... and ζ_M, the basis used to represent uncertain model parameters. Various types orthogonal polynomial functions can be used for H_k in Eq. (8) depending on the nature of the uncertain parameters being considered.

In practice, Eq. (8) is truncated at a finite order for ease of implementation. For the uncertain parameters considered in this work, second-order polynomials were sufficient to approximate their probability distributions with reasonable accuracy. The coefficients a_k of the expansion were computed by evaluating the process model at collocation points specific to the probability distributions of model parameters. The number of model evaluations required to compute the unknown coefficients depends on the number of uncertain parameters and the number of terms used in the polynomial chaos expansion. This number is of the same order as the number of uncertain parameters thus is much smaller than needed by Monte Carlo simulation. DEMM has proven capable of closely approximating the results of Monte Carlo simulation with significantly reduced computational time, often 2-3 orders of magnitude less [13, 14, 15, 16, 17].

Sensitivity analysis

DEMM also provides direct means of evaluating the sensitivity of model output to parametric uncertainties and identifying the parameters contributing the most to output uncertainty. Parametric sensitivities, defined as the portion of variance of model output that is attributable to individual parameters, are readily computable upon obtaining the coefficients of polynomial chaos expansion from Eq. (8). Assume the model output y is approximated by second-order polynomial functions of M Gaussian parameters, neglecting cross product terms

$$y = a_0 + \sum_{k=0}^{M} [a_{2k-1}\zeta_k + a_{2k}(\zeta_k^2 - 1)] \tag{9}$$

The variance of y is computed based on Eq. (9) as follows

$$var[y] = E[(y - E[y])^2] = \sum_{k=0}^{M} (a_{2k-1}^2 + 2a_{2k}^2) \tag{10}$$

Evaluation of the variance makes use of orthogonality of Hermite polynomials and the following properties of standard Gaussian random variable

$$E[\zeta^n] = \begin{cases} 0 & n = 2k-1 \\ 1 \cdot 3 \cdot 5 \cdot ...(n-1) & n = 2k, \quad k = 1, 2, ..., M \end{cases} \tag{11}$$

The portion of variance attributable to j-th (j = 1, 2, ..., M) parameter is clearly seen from Eq. (12)

$$var[y]|_{\zeta_j} = a_{2j-1}^2 + 2a_{2j}^2 \tag{12}$$

This highlights the parameters where reduction in uncertainty would most effectively improve the predictive performance of the model. Those with negligible contribution to overall uncertainty can be phased out from further analysis.

3. Results and discussion

3.1. Uncertain input parameters

17 uncertain input parameters were selected for the analysis, as displayed in Table 2. The pressure drop $\Delta p/p$ was simply modeled as being the same for all equipment in the system. This means, for example, that the ATR was modeled with the same pressure drop (%) as the LTS. The steam-to-carbon ratio (S/C) is the moles of steam per moles of fuel carbon admitted to the reforming section. T_A is the temperature approach for reaction (3) in the HTS and LTS respectively. Parameters 5 and 6 represent the air booster compressor isentropic efficiency η_{boost} and pressure ratio PR_{boost}. The turbine inlet temperature (TIT) for the gas turbine set was an uncertain input parameter to the model. The full TIT for the GE 9FB GT is 1427 °C, however, the IGCC setup of the 9FB includes replacing the hot gas path of the FB with FA parts. The 9FA design turbine inlet temperature is 1327 °C. Also, because of the hydrogen fuel which leads to an increase in steam content in the turbine compared to when firing natural gas, the heat transfer rate to the turbine blades increases, leading to a higher blade metal temperature. The TIT reduction necessary to compensate for this is uncertain. Chiesa et al. [18] report TIT reductions of 10-45 K. A 50 K range of the TIT reduction was selected for the uncertainty analysis. GT PRO allows for altering the polytropic

Table 2: Input uncertain parameters for IRCC process: nominal values and probability distributions

No.	Sub-system	Variable	Distribution	Central value	Lower bound	Max likeli-hood	Upper bound	Mean	St. dev.
1	All	$\Delta p/p$ (%)	Uniform	2.25	0.5		4		
2	Reforming	S/C	Normal	1.5				1.5	0.03
3	WGS	$T_{A,HTS}$ (K)	Uniform	10	0		20		
4		$T_{A,LTS}$ (K)	Uniform	5	0		10		
5	Booster comp	η_{boost}	Triangular	0.85	0.8	0.85	0.9		
6		PR_{boost}	Triangular	1.918	1.82	1.918	2.02		
7	Gas turbine	TIT ($^{\circ}$C)	Uniform	1302	1277		1327		
8		$\Delta\eta_c$ (%-point)	Triangular	0	-2	0	2		
9		$\Delta\eta_t$ (%-point)	Triangular	0	-2	0	2		
10	Steam turbine	$CF_{\eta,HP}$	Triangular	1	0.95	1	1.05		
11		$CF_{\eta,LP}$	Triangular	1	0.95	1	1.05		
12	CO_2 capture	W_{re} (MJ/kg)	Uniform	2.0	1.8		2.2		
13	CO_2 comp	$\eta_{CO2,1}$	Triangular	0.85	0.8	0.85	0.9		
14		$\eta_{CO2,2}$	Triangular	0.8	0.75	0.8	0.85		
15		$\eta_{CO2,3}$	Triangular	0.8	0.75	0.8	0.85		
16		$\eta_{CO2,4}$	Triangular	0.75	0.7	0.75	0.8		
17		η_p	Triangular	0.7	0.65	0.7	0.75		

efficiencies for the GT compressor and turbine for a set model selection. This modification of efficiency is termed $\Delta\eta$. In addition, a correction factor, CF_η for the LP and HP steam turbine isentropic efficiencies was used. For the CO_2 capture sub-system the reboiler duty W_{re} was deemed uncertain. Parameters 13-17 are the isentropic efficiencies for the 4-stage compression system and the following pump.

The distribution of each variable and the associated values of the distribution were selected in consultation with technical experts. The selected distributions reflected the best knowledge of the experts in an unbiased way. For instance, the percentage pressure drop $\Delta p/p$ was believed to vary within the vicinity of 2%. Careful assessment determined it might vary between 0.5% and 4% but it was not evident that any value in between was more likely than others. A uniform distribution on [0.5%, 4%] was derived, based on the maximum entropy principle, in order to avoid biasing the available information. Similarly, the isentropic efficiency of the air booster was believed to be 0.85 with high confidence and the largest possible variation was ± 0.05. A triangular distribution was justifiable in this case. The probability distributions of three variables, steam-to-carbon ratio, isentropic efficiency of air booster and turbine inlet temperature, are graphically shown in Fig. 3 (a). Second-order polynomial chaos expansion was used to approximate uncertainties in model response variables. For the IRCC model with 17 uncertain variables, DEMM required 35 executions of the process model.

3.2. Uncertain model outputs

Uncertainties in all 17 input variables were propagated through the IRCC model using DEMM to estimate uncertainties in four key performance metrics:

- net plant power output

- net plant efficiency

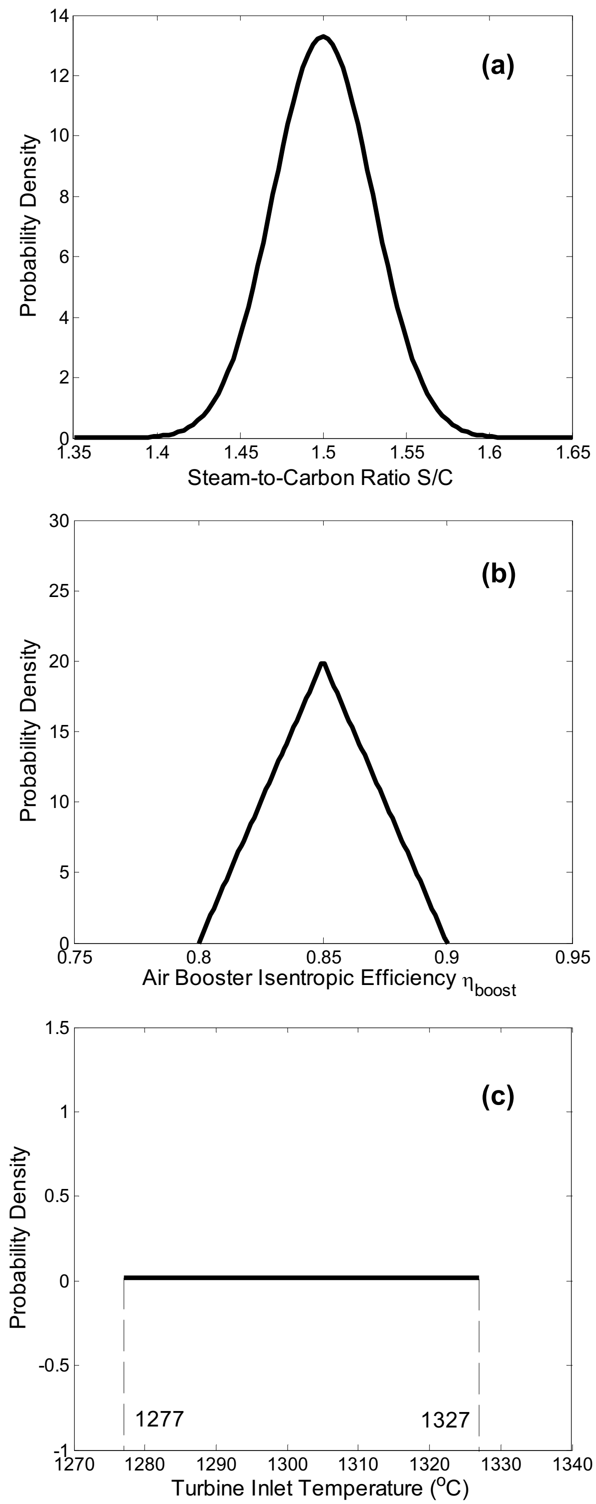

Figure 3: Probability distributions of (a) steam-to-carbon ratio, (b) isentropic efficiency of air booster and (c) turbine inlet temperature as estimated from experts' knowledge regarding their respective uncertainties.

- CO_2 capture rate
- CO_2 emitted

All results reported are based on a plant size of approximately 350 MW. The GT inlet air mass flow and TIT were kept constant during the simulation runs (except during the TIT sensitivity cases where TIT was varied). The results are shown both in terms of probability density function (pdf) and cumulative probability function (cdf). The pdf describes the density of probability at each point in the range of an uncertain variable. It shows the shape of the probability distribution as well as many probabilistic characteristics, such as maximum likelihood value, and skewness and peakness. The cdf is the integral of probability density function. It gives the probability of a variable being equal to or less than a given value. One less the cumulative probability is the probability of exceeding the corresponding value. The pdf and cdf each represent a complete description of the probability distribution of an uncertain variable. However, they also emphasize different features of the distribution and thus complement each other in displaying an uncertain variable.

The net plant power output was defined as:

$$\dot{W}_{net,plant} = ((\dot{W}_t - \dot{W}_c) + \dot{W}_s)\eta_m\eta_{gen} - (\dot{W}_{comp} + \dot{W}_p)/(\eta_m\eta_{drive}) - \dot{W}_{aux} \quad (13)$$

where $\dot{W}_t$ is the GT turbine power, $\dot{W}_c$ the GT compressor power, $\dot{W}_s$ the ST power, $\dot{W}_{comp}$ the total power consumption by the air and CO_2 compression. $\dot{W}_p$ is the pump power in the absorption sub-system. $\dot{W}_{aux}$ is the auxiliary power requirement. η_m is the mechanical efficiency and η_{gen} is the generator efficiency. η_{drive} is the efficiency of the drives for the different compressors and pumps. Note that all the power terms were defined as their absolute values meaning all power terms were considered positive and the sign handled in the equation itself. The predicted uncertainty of net plant power output is shown in Fig. 4. The deterministic model prediction, based on best estimates of all model input parameters, is plotted as a dash-dotted line.

The pdf plot in Fig. 4 shows the predicted net power output ranged from 322 MW to 384 MW with a standard deviation of 9.4 MW. The median value, or 50th percentile, was 352.7 MW which is almost equal to the deterministic prediction 352.9 MW. There is about equal chance that the net power output exceeds or falls short of the deterministic prediction. This is primarily attributable to the assumed uniformly distributed turbine inlet temperature which is shown to account for 75% of the uncertainty in net power output. More details of parametric sensitivities are shown in Table 3 and discussed in Section 3.3. The shape of the distribution is another illustration of the prominent impact of turbine inlet temperature on predicted net power output. The pdf curve has steep tails on both sides and plateaus between 344 MW and 362 MW, approximately a standard deviation away from the median. The uniformity of the distribution of turbine inlet temperature to a large extent translates to that of the distribution of net power output.

Although the deterministic value was roughly the same as the predicted median value, the uncertainty estimates in Fig. 4 point out that in the worst case scenario, the net power output could drop to as low as 322 MW, 8.5% lower than the deterministic value. This downside risk is inherent with the model as a result of incomplete knowledge and will not be eliminated unless additional research is taken to reduce uncertainties in input parameters. This exemplifies the inability of deterministic simulation in understanding the risk associated with process performance. Failure to do so may expose the decision-makers to undesired consequences.

Another key performance metrics was the net plant efficiency which was defined as

$$\eta_{net,plant} = \frac{\dot{W}_{net,plant}}{(\dot{m}LHV)_{NG}} \tag{14}$$

where $\dot{m}_{NG}$ is the natural gas mass flow entering the system and LHV_{NG} the lower heating value of the natural gas. As shown in Fig. 5 (a), the net plant efficiency had a median of 43.4%, equal to the deterministic value. It could vary within a narrow range between 41.8% and 45.2%, resulting in a small standard deviation of 0.5%. The total variability was a mere 7.8% of the median value, indicating high confidence of the model in predicting net plant efficiency. It is noteworthy that the net plant efficiency has a smaller relative uncertainty, the ratio of standard deviation to median, than the net power output. This can be understood through examination of the definition (14). Given the lower heating value is known with certainty, the plant efficiency depends on both net power output and mass flow of natural gas fed to the system. The latter was allowed to vary so as to maintain the turbine inlet temperature at desired level. As is evident from parametric sensitivity results shown in Table 3, the TIT has the most significant influence on the plant efficiency. An increase in TIT would require larger inlet flow of natural gas and leads to larger power generation and vice versa. Thus, the mass flow of natural gas varies in the same direction as the net power output and to some extent offsets the uncertainty of the latter.

CO_2 capture rate and CO_2 emitted are two closely related parameters. The CO_2 capture rate was defined as the fraction of formed and fuel CO_2, $\dot{m}_{CO2,form}$ and $\dot{m}_{CO2,fuel}$, that is captured $\dot{m}_{CO2,cap}$ (on a mass flow basis)

$$CO_2\, capture\, rate = \frac{\dot{m}_{CO2,cap}}{\dot{m}_{CO2,form} + \dot{m}_{CO2,fuel}} \tag{15}$$

The CO_2 emitted was defined as the mass of carbon dioxide emitted in the power plant stack, $m_{CO2,emi}$, per kWh of net plant electricity output $W_{net,plant}$

$$CO_2\, emitted = \frac{m_{CO2,emi}}{W_{net,plant}} \qquad \left(\frac{g}{kWh}\right) \tag{16}$$

The pdf in Fig. 6 (a) shows rather small uncertainty in the CO_2 capture rate. The median was 85.5% and with about 90% probability the model predicted a capture rate between 85% and 86%. Furthermore, as seen in Fig. 6 (b), the probability of meeting the requirement of at least 85% capture rate was approximately 95%. The pdf and cdf of CO_2 emitted are displayed in Fig. 7. The median was 70.6 g/kWh, which was slightly

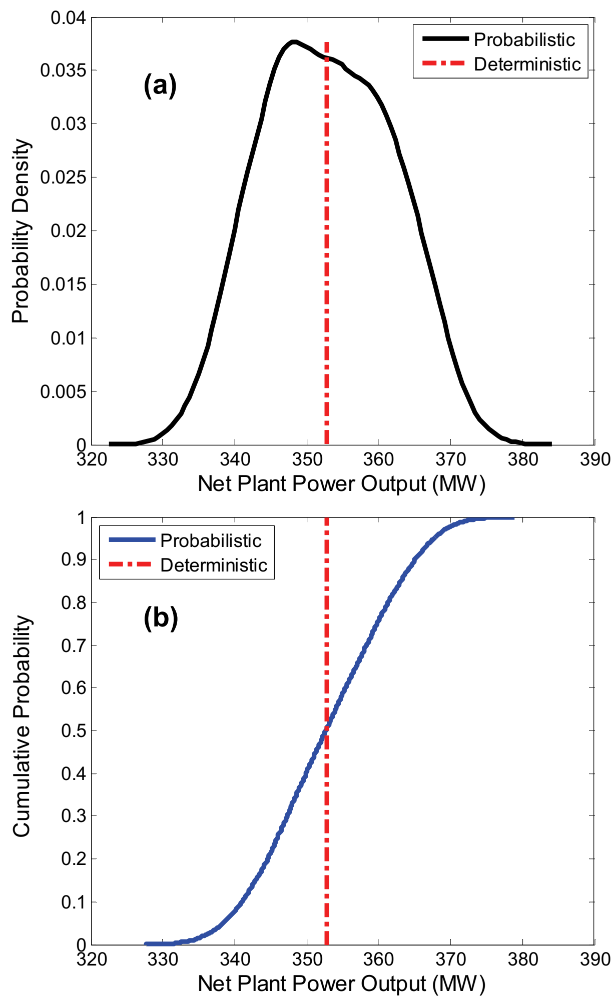

Figure 4: Predicted probability distribution of net plant power output from polynomial approximation obtained via DEMM. The results are shown as (a) probability density function, (b) cumulative probability function. The solid lines represent probability distribution and the vertical dash-dotted line is the deterministic prediction.

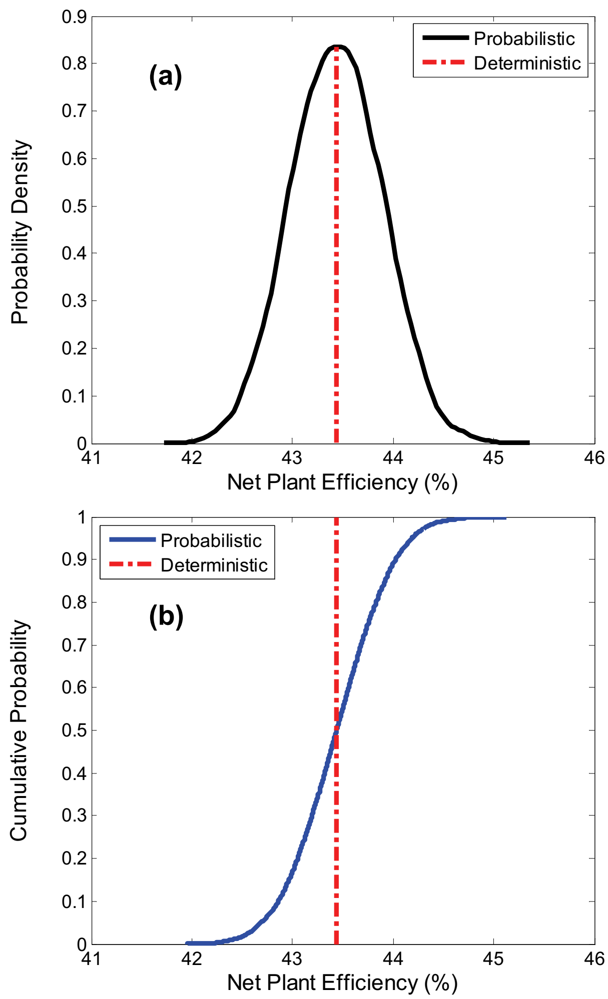

Figure 5: Predicted probability distribution of net plant efficiency from polynomial approximation obtained via DEMM. The results are shown as (a) probability density function, (b) cumulative probability function. The solid lines represent probability distribution and the vertical dash-dotted line is the deterministic prediction.

Table 3: Key input parameters for performance metrics. The contributions to the total variance are expressed as percentage.

Net Power Output		Net Plant Efficiency		CO_2 Capture Rate		CO_2 Emitted	
Parameter	Sensitivity	Parameter	Sensitivity	Parameter	Sensitivity	Parameter	Sensitivity
TIT	74.5%	TIT	24.7%	$\Delta p/p$	53.7%	$\Delta p/p$	58.8%
$\Delta\eta_c$	9.6%	$\Delta\eta_t$	22.7%	S/C	27.9%	S/C	14.5%
$\Delta p/p$	7.6%	$\Delta p/p$	14.1%	$T_{A,LTS}$	13.1%	$T_{A,LTS}$	9.1%
$\Delta\eta_t$	3.8%	$CF_{\eta,LP}$	12.2%	PR_{boost}	3.3%	$\Delta\eta_t$	3.8%
$CF_{\eta,LP}$	2.0%	$\Delta\eta_c$	11.0%	$T_{A,HTS}$	1.2%	$\Delta\eta_c$	3.3%
W_{re}	1.6%	W_{re}	9.5%			PR_{boost}	2.8%
		S/C	2.8%			TIT	2.5%
		$CF_{\eta,HP}$	2.5%			$CF_{\eta,LP}$	2.0%
						W_{re}	1.6%
Subtotal	99.0%		99.4%		99.2%		98.4%

lower than the deterministic value 70.9 g/kWh. The difference was smaller than the estimated standard deviation of 1.9 g/kWh and thus should be considered insignificant. The shape of the pdf curves of both CO_2 capture rate and CO_2 emitted resembled that of normal distribution but with heavy tails on both sides of the median. It reflects the large influence of $\Delta p/p$ and steam-to-carbon ratio (S/C), which were assumed as uniform and normal distributions respectively, on the output uncertainty. This is shown in Table 3. The flat distributed $\Delta p/p$ raises the probability of both outputs deviating from their median values.

3.3. Key uncertain input parameters

Using the polynomial approximation to the model output, the sensitivity of the output to input uncertainties can be directly evaluated and key parameters that drive the uncertainty in model performance be identified. The contribution to total variance by individual parameters was computed using Eq. (12). The parameters which account for over 1% variance of the performance metrics are summarized in Table 3.

Turbine inlet temperature (TIT) is a critical parameter in relation to gas turbine performance. A higher TIT leads to a higher thermal efficiency of the GT. In addition, the exhaust temperature increases with an increased TIT leading to a higher steam production in the HRSG. As listed in Table 3, TIT had the biggest influence on the uncertainty of the net plant efficiency. Another important parameter is the polytropic turbine efficiency since it also changes the GT efficiency *and* the GT exhaust temperature (although in "different" directions since an increase in turbine efficiency increases overall GT efficiency but decreases exhaust temperature). These two parameters together contribute to over 45% of the variance.

As mentioned, TIT effects the GT efficiency and exhaust temperature. In addition, a change in TIT alters the GT power output. The compounded effect resulted in a clear dominance of TIT to net power output uncertainty as evident in Table 3. For example, an increase in TIT would lead to:

- an increase in GT thermal efficiency meaning a higher power output for a given fuel input
- an increase in power output due to an increase in fuel mass flow (a higher fuel mass flow is needed to reach a higher TIT for a given air mass flow)
- an increase in GT exhaust temperature enabling generation of more steam for ST

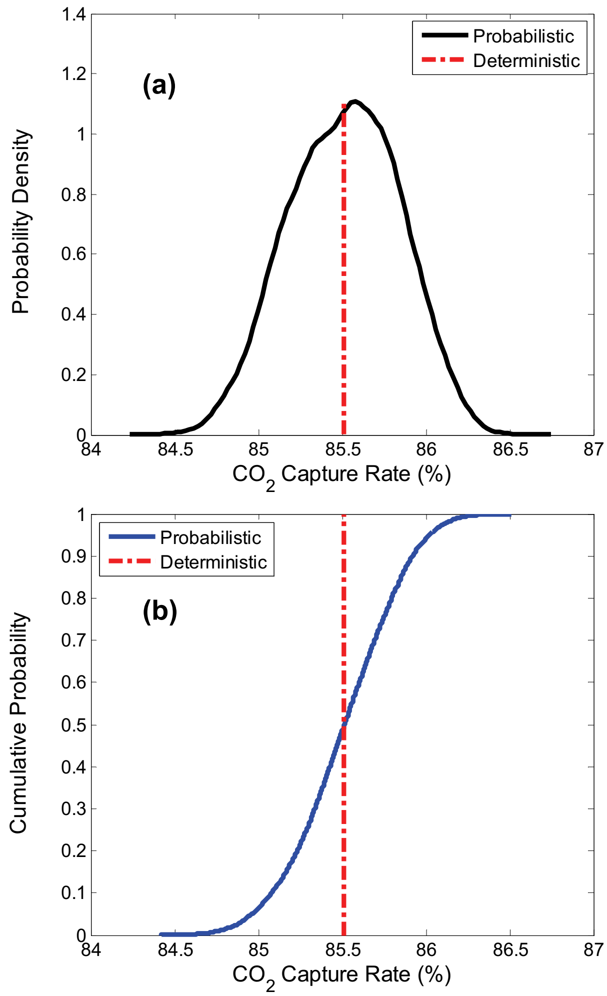

Figure 6: Predicted probability distribution of CO_2 capture rate from polynomial approximation obtained via DEMM. The results are shown as (a) probability density function, (b) cumulative probability function. The solid lines represent probability distribution and the vertical dash-dotted line is the deterministic prediction.

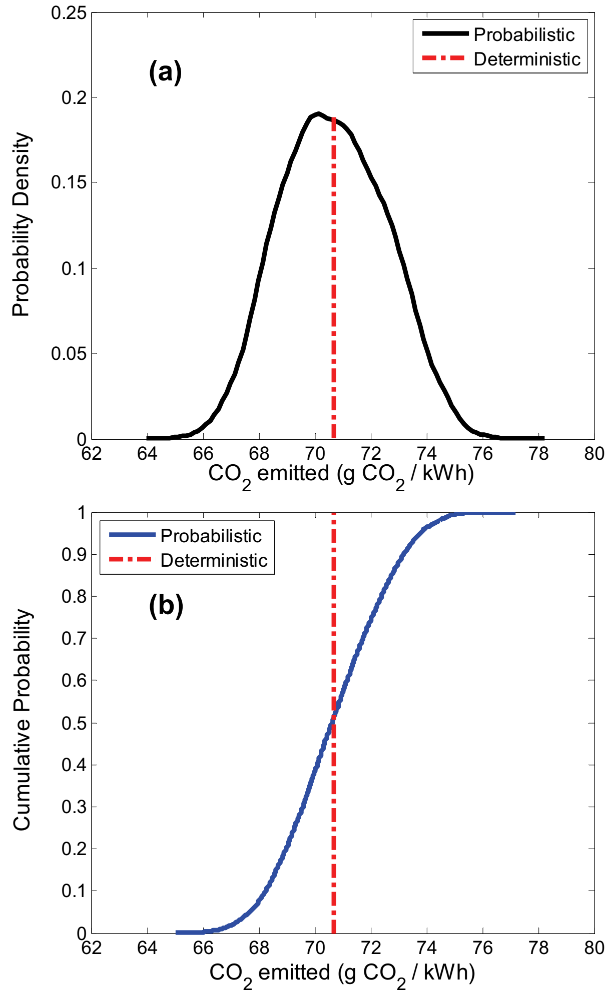

Figure 7: Predicted probability distribution of CO_2 emitted from polynomial approximation obtained via DEMM. The results are shown as (a) probability density function, (b) cumulative probability function. The solid lines represent probability distribution and the vertical dash-dotted line is the deterministic prediction.

Table 4: Input uncertain parameters for NGCC process: nominal values and probability distributions

No.	Sub-system	Variable	Distribution	Value	Lower bound	Max likelihood value	Upper bound
1	Gas Turbine	$\Delta\eta_c$ (%-point)	Triangular	0	-1	0	1
2		$\Delta\eta_t$ (%-point)	Triangular	0	-1	0	1
3	Steam turbine	$CF_{\eta,HP}$	Triangular	1	0.95	1	1.05
4		$CF_{\eta,LP}$	Triangular	1	0.95	1	1.05

Not surprisingly, TIT accounted for about 75% of the variance of net power output. It should be mentioned that a rather wide TIT input uncertainty distribution was chosen, as listed in Table 2. By selecting a narrower range, the TIT dominance on output uncertainty would not be as pronounced.

CO_2 capture rate and CO_2 emitted, though not quite as uncertain, were dictated by different sets of parameters among which pressure drop and steam-to-carbon ratio were the most prominent. The pressure drop variation runs were done by keeping the fuel pressure to the GT constant and varying each equipment's Δp. This means that the reformer pressure will vary significantly with changes in the pressure drop parameter. For example, by varying $\Delta p/p$ from 2.25% to 4%, the ATR outlet pressure changed from 30.6 bar to 35.4 bar. This shifted the equilibrium in the reforming reaction (5) to the left leading to a higher methane slip from the reformer. This CH_4 will be passed on to the GT combustor and thereby increasing the CO_2 content in the GT exhaust. The capture rate would then go down and the CO_2 emitted increase. In addition to the reforming pressure, the S/C is a critical reforming and water-gas shift parameter (refer to reactions (1) through (5)). A higher S/C decreases the CO_2 emitted (but also decreases the cycle efficiency). For both the CO_2 capture rate and CO_2 emitted the S/C and pressure drop combined contribution was over 70% on output variance, as can be seen in Table 3.

3.4. Comparison to reference case

Comparative study plays an important role in evaluation of design trade-offs and competing technologies. The preceding sections have shown that predictions of performance by no means are free of uncertainties. Comparison based on probabilistic estimates often provides critical insights that could be overlooked by deterministic approach. The concept of technology comparison under uncertainty is illustrated with a reference case consisting of a natural gas combined cycle (NGCC) system where CO_2 capture is not employed. The reference case included the same type GT and a triple-pressure steam bottoming cycle. The objective was to assess the efficiency penalty, that is, how many %-points in net plant efficiency were lost by including CO_2 capture.

Input parameters for NGCC model were selected by virtue of technical experts' knowledge in a similar way to the IRCC case, as shown in Table 4. The predicted pdfs of the net plant efficiency for the NGCC reference case and the IRCC model are displayed in Fig. 8. It is clear that the performance of the IRCC was more uncertain than that of the NGCC. This is partly because NGCC technology is much more mature than IRCC technology. Furthermore, an IRCC plant is more complex than an NGCC plant and thus increasing

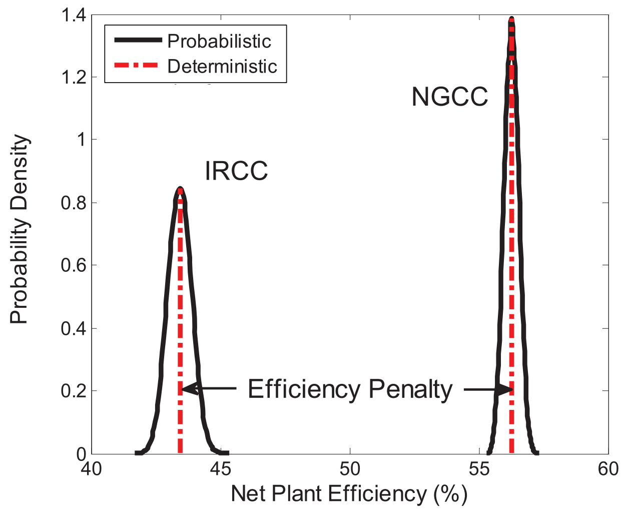

Figure 8: Predicted probability distribution of net plant efficiency for the NGCC reference plant and the IRCC plant. The solid lines represent probability distribution and the vertical dash-dotted line is the deterministic value.

model output uncertainties. The median efficiency was 56.3% for NGCC and 43.4% for IRCC, resulting in a difference of 12.8%-points, which was same as the efficiency penalty computed by deterministic analysis. However the uncertain nature of predicted efficiency of both processes makes the efficiency penalty uncertain. In other words, the efficiency loss caused by capturing CO_2 may be more significant than the deterministic analysis indicated. A plot of the probability distribution of the efficiency penalty provides more insight on the effect of CO_2 capture, as displayed in Fig. 9. In general, the uncertainty in the difference of two variables cannot straightforwardly be derived from their marginal distributions, especially when they share common uncertainties. The comparison based on the polynomial representations of parametric uncertainties took into account the underlying correlation structure.

The median of efficiency penalty was 12.8%-points, but it could rise to as high as 14%-points in the worst case scenario. From the cumulative probability plot in Fig. 9 (b), there was about 51% probability that actual efficiency penalty could exceed the deterministic value. This observation is more remarkable than it appears, meaning deterministic analysis would underestimate the efficiency penalty with over 50% chance.

4. Conclusions

An integrated approach to characterizing uncertainties has allowed the evaluation of key performance and environmental control metrics such as net power output, net plant efficiency, and projected CO_2 emissions, that are affected by several model input uncertainties. Being able to not only predict the likely values of process performance but place confidence limits on the predictions is essential to making informed decisions on technology evaluation.

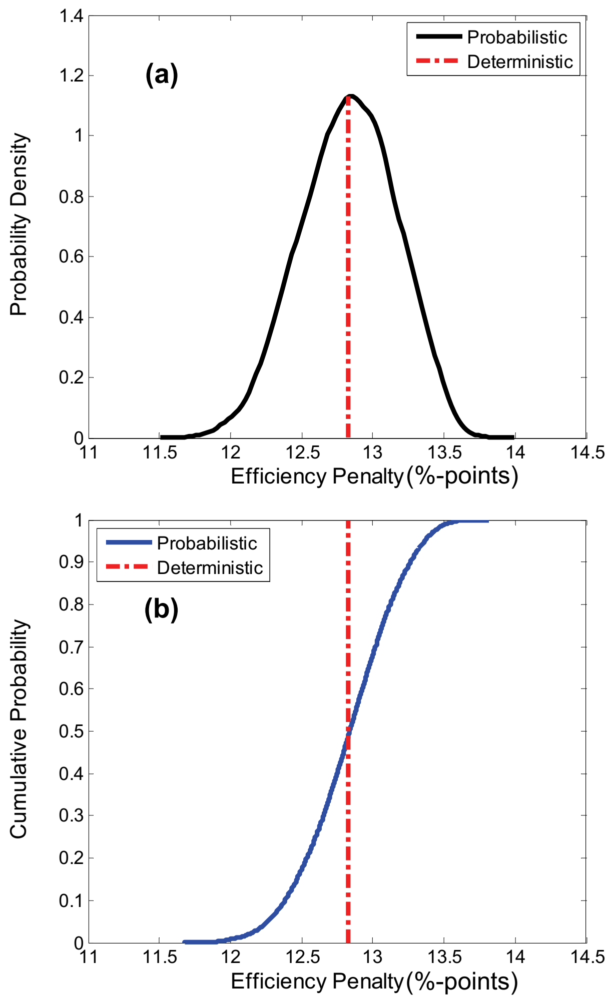

Figure 9: Probability distribution of efficiency penalty, the difference in net efficiencies of an NGCC plant and an IRCC plant. The solid lines represent probability distribution and the vertical dash-dotted line is the deterministic value.

By explicitly characterizing parametric uncertainties of an IRCC plant with CO_2 capture, it was found that the net power output from the IRCC plant may incur large uncertainty which primarily is attributable to the uncertain behavior of the gas turbine. Improvement of confidence in the prediction of power output can be achieved by reducing the uncertainty in the estimate of turbine inlet temperature. Fortunately, the model was able to predict the net plant efficiency with relatively high precision. Furthermore, the plant was projected to meet the requirement of 85% CO_2 capture rate with 95% confidence.

DEMM has proven to be a computationally efficient method for propagating multiple uncertainties through complex flowsheets, in this case an IRCC process model. It would have been unrealistic to run thousands of simulations for such a model, as would be necessary with a Monte Carlo approach, not the least because the model is linked between different simulation packages. In addition, DEMM enables the evaluation of the sensitivity of input uncertainties. Such results can help highlight the parameters where reduction of uncertainty via additional research can most effectively improve confidence in model predictions. Uncertainty analysis should be an integral part of evaluation of advanced power plant with CO_2 capture during the planning and design stage. It is likely to have significant implication to subsequent decision-making regarding research planning, risk management, and capital investment.

5. Acknowledgments

The authors gratefully acknowledge financial support from the Norwegian Research Council and Statoil-Hydro through the MIT Energy Initiative.

References

[1] H. C. Frey, E. S. Rubin, Evaluation of advanced coal gasification combined-cycle systems under uncertainty, Industrial Engineering & Chemistry Research 31 (1992) 1299–1307.

[2] H. C. Frey, E. S. Rubin, Integration of coal utilization and environmental control in integrated gasification combined cycle systems, Environmental Science & Technology 26 (1992) 1982–1990.

[3] U. M. Diwekar, E. S. Rubin, Stochastic modeling of chemical processes, Computers & Chemical Engineering 15 (2) (1991) 105–114.

[4] C. Chen, E. S. Rubin, CO_2 control technology effects on IGCC plant performance and cost, Energy Policy 37 (2009) 915–924.

[5] T. Andersen, H. M. Kvamsdal, O. Bolland, Gas turbine combined cycle with CO_2 capture using auto-thermal reforming of natural gas, in: ASME Turbo Expo, Munich, Germany, 2000.

[6] G. Lozza, P. Chiesa, Natural gas decarbonization to reduce CO_2 emission from combined cycles - part I: partial oxidation, Journal of Engineering for Gas Turbines and Power 124 (1) (2002) 82–88.

[7] G. Lozza, P. Chiesa, Natural gas decarbonization to reduce CO_2 emission from combined cycles - part II: steam-methane reforming, Journal of Engineering for Gas Turbines and Power 124 (1) (2002) 89–95.

[8] A. Corradetti, U. Desideri, Analysis of gas-steam combined cycles with natural gas reforming and CO_2 capture, Journal of Engineering for Gas Turbines and Power 127 (3) (2005) 545–552.

[9] I. S. Ertesvåg, H. M. Kvamsdal, O. Bolland, Exergy analysis of a gas-turbine combined-cycle power plant with precombustion CO_2 capture, Energy 30 (1) (2005) 5–39.

[10] S. Hoffmann, M. Bartlett, M. Finkenrath, A. Evulet, T. P. Ursin, Performance and cost analysis of advanced gas turbine cycles with precombustion CO_2 capture, Journal of Engineering for Gas Turbines and Power 131 (2) (2009) 021701 (7 pp.).

[11] L. O. Nord, R. Anantharaman, O. Bolland, Design and off-design analyses of a pre-combustion CO_2 capture process in a natural gas combined cycle power plant, International Journal of Greenhouse Gas Control 3 (4) (2009) 385–392.

[12] A. Golan, G. Judge, D. Miller, Maximum entropy econometrics : robust estimation with limited data, Wiley, New York, 1996.

[13] M. A. Tatang, Direct incorporation of uncertainty in chemical and environmental engineering systems, Ph.D. thesis, Massachusetts Institute of Technology, Cambridge, MA (1995).

[14] M. A. Tatang, W. Pan, R. G. Prinn, G. J. McRae, An efficient method for parametric uncertainty analysis of numerical geophysical models, Journal of Geophysical Research 102 (1997) 21916–21924.

[15] B. D. Phenix, J. L. Dinaro, M. A. Tatang, J. W. Tester, J. B. Howard, G. J. McRae, Incorporation of parametric uncertainty into complex kinetic mechanisms: application to hydrogen oxidation in supercritical water, Combustion and Flame 112 (1998) 132–146.

[16] Y. Chen, G. J. McRae, K. K. Gleason, Directly addressing uncertainty in esh evaluation, in: Electronics and the Environment: Proceedings of the IEEE International Symposium, 2005, pp. 31–35.

[17] B. Gong, L. Duan, R. Field, G. J. McRae, Evaluation of integrated gasification combined cycle processes under technological and economical uncertainties, to be submitted.

[18] P. Chiesa, G. Lozza, L. Mazzocchi, Using hydrogen as gas turbine fuel, Journal of Engineering for Gas Turbines and Power 127 (1) (2005) 73–80.